Effect of soluble surfactant on regime transitions at drop formation

Kovalchuk, Nina M.; Simmons, Mark J.h.

DOI:
10.1016/j.colsurfa.2018.02.041

Document Version
Publisher's PDF, also known as Version of record

Citation for published version (Harvard):
Kovalchuk, NM & Simmons, MJH 2018, 'Effect of soluble surfactant on regime transitions at drop formation', *Colloids and Surfaces A: Physicochemical and Engineering Aspects*, pp. 1-7.
https://doi.org/10.1016/j.colsurfa.2018.02.041

Colloids and Surfaces A 545 (2018) 1–7

Contents lists available at ScienceDirect

Colloids and Surfaces A

journal homepage: www.elsevier.com/locate/colsurfa

Effect of soluble surfactant on regime transitions at drop formation

Nina M. Kovalchuk*, Mark J.H. Simmons

School of Chemical Engineering, University of Birmingham, Edgbaston, B152TT, Birmingham, UK

GRAPHICAL ABSTRACT

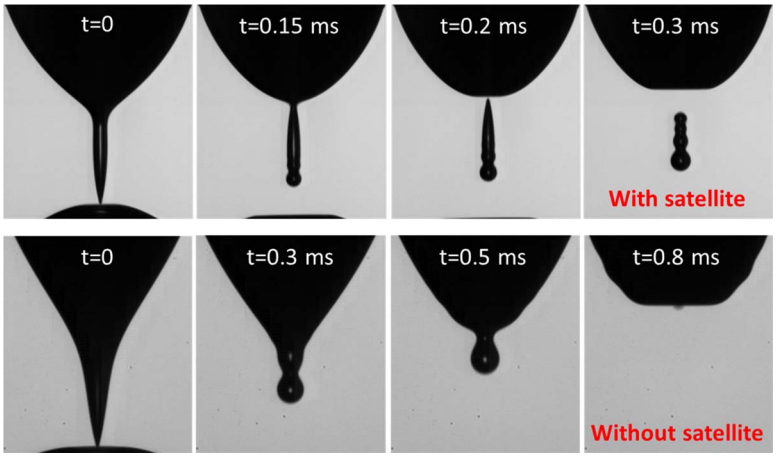

ARTICLE INFO

Keywords:
Drop formation
Pinch-off
Flow rate
Dynamic surface tension
Critical micelle concentration
Satellite droplet
Dripping to jetting transition

ABSTRACT

Formation of surfactant-laden aqueous drops by liquid flow through a capillary is studied and compared with two reference pure liquids, water and low viscosity poly(dimethylsiloxane). Attention is paid to two transitions: (i) between regimes with and without satellite droplet formation and (ii) from dripping to jetting. It is shown that transition from dripping to jetting occurs at critical Weber number $We_J = 1.2 \pm 0.1$ based on dynamic surface tension on the flow timescale. Critical Weber number for transition to the regime without satellite droplets depends noticeably on the liquid surface tension and therefore cannot be used as a single parameter characterising this transition. Flow rate at transition decreases with decrease of surface tension for pure liquids and solutions of surfactants with critical micelle concentration, CMC $>$ 10 mM. For solutions of surfactants with CMC $<$ 1 mM transition to the regime without satellite droplets occurs at flow rates either larger or smaller than that of pure solvent depending on concentration. Anomalously high transition flow rates are related to surfactant redistribution during the time between the primary and secondary pinch-off.

1. Introduction

Drop formation is broadly used in industry: emulsification, spraying and ink jet printing are a few examples of the numerous applications which currently exist. Typical drop sizes required cover several orders of magnitude from micrometres to millimetres and the corresponding time scales of formation cover the range from sub-milliseconds to seconds. At small flow rates, liquid drops are formed in the dripping

* Corresponding author.
E-mail address: n.kovalchuk@bham.ac.uk (N.M. Kovalchuk).

https://doi.org/10.1016/j.colsurfa.2018.02.041
Received 14 December 2017; Received in revised form 16 February 2018; Accepted 16 February 2018
Available online 17 February 2018

regime, when the time interval between subsequent drops is constant and drop size distribution is narrow. In what follows this regime is called a stationary dripping. As the flow rate increases, the drop formation becomes less regular with transition to regime called chaotic dripping [1] or dripping faucet [2]. Finally transition to jetting regime occurs where drops are formed due to the Rayleigh instability [1–4]. One more transition takes place inside the dripping regime. At small flow rates, formation of the main drop is accompanied by formation of a small satellite droplet, which is suppressed at larger flow rates [4–7].

Precise criteria for these transitions are vital for most applications, because transitions affect drop size and size distribution, determine the optimal throughput for a drop formation process and product quality. For example, technologies enabling avoidance of satellite droplets formation are of great demand in ink jet printing [8] and in spray-drying [9], because satellites or fines can be easily misdirected by electric field or air flow and therefore can considerably reduce the quality of final product. Another example is production of hydrogel capsules for 3-D cell culture, where capsules of mm-size were produced in dripping mode [10], whereas those of sub-mm size were produced in the jetting mode [11].

The behaviour of liquid flowing out of a nozzle is completely characterised by four dimensionless numbers [5,6], namely Weber number,

$$We = \rho u^2 R_{in}/\sigma = \rho Q^2/\pi^2 \sigma R_{in}^3 \quad (1)$$

Ohnesorge number,

$$Oh = \mu/\sqrt{\rho \sigma R_{out}} \quad (2)$$

gravitational Bond number,

$$Bo = \Delta\rho g R_{out}^2/\sigma \quad (3)$$

and the ratio of inner and outer nozzle radius R_{in}/R_{out}, where u is the liquid velocity, σ is the surface tension, Q is the flow rate, μ is the dynamic viscosity of liquid, $\Delta\rho$ is the density difference between the liquid in the drop and ambient fluid ($\Delta\rho \sim \rho$, liquid density, if the ambient fluid is air) and g is the acceleration due to gravity [1]. If $R_{in}/R_{out} > 0.5$ the effect of the wall thickness on the dynamics of the process can be neglected [12].

The transition from dripping to jetting, which in fact is a transition from absolute to convective instability was intensively studied for pure liquids both theoretically and experimentally and summary of most important results is given in Ref. [1].

Thorough studies on the formation of satellite droplets during dripping of surfactant-free liquids have been published [5–7,12,13] including both numerical simulations and experiments. The behaviour of a satellite drop is determined by recoiling speed of the bridge after primary pinch-off and the rate of secondary pinch-off. During dripping from thin capillaries it is noted that the speed of recoil is sufficiently large to repress secondary pinch-off thus no satellite droplet is formed. An increase in the capillary size results in formation of a satellite drop moving upward and often coalescing with the liquid remaining on the capillary. At further increase of capillary size, the upward motion of the satellite slowed down and after a certain threshold capillary size the satellites moving downward were observed [12]. Suppression of satellite formation due to an increase of flow rate was not observed in this study due to flow rate limitations, but was predicted in numerical simulations and found experimentally in subsequent studies [5–7].

In line with Ref. [12] it was found in Ref. [7] that the ratio of inner and outer capillary diameter is an important parameter for formation of the satellite drops, which are formed only if this ratio exceeds 0.48. If this is the case the transition to the regime where formation of satellite drops is suppressed is determined by Weber number and depends much less upon Bond number. From analysis of numerical and experimental data for the drops of pure water ($Oh << 1$) a parameter

$$K = We \cdot Bo^{0.3921} \quad (4)$$

was proposed to best characterise this transition. Satellite droplets cease to form at $K > 0.0125$ [7]. In the more general case, the critical Weber number for transition to regime without satellite droplets depends also on Ohnesorge number [6].

Despite a very broad use of surfactants in industrial processes involving drop formation, there are relatively few publications focussing on surfactant-laden rather than surfactant free drops, with most attention paid to kinetics of drop formation and the size of satellite drops [12,14–19]. The effect of soluble surfactant on the dripping to jetting transition and the transition to regime without satellite drops has not been considered in the published literature. The work presented in this paper addresses this issue using a series of cationic surfactants, alkyltrimethylammonium bromides with chain length C10-C16.

2. Experimental

The surfactants, decyltrimethylammonium bromide (C_{10}TAB), Acros organics, 99%; dodecyltrimethylammonium bromide (C_{12}TAB), Acros organics, 99%; hexadecyltrimethylammonium bromide (C_{16}TAB), Sigma, BioXtra, ≥99%; as well as sodium bromide, Sigma, BioUltra, ≥99.5% and Poly(dimethylsiloxane) (PDMS), Sigma, density 820 kg/m^3, were used as purchased. All solutions in concentration range from 0.2 to 10 critical micelle concentrations (CMC) were prepared in double-distilled water produced by water still Aquatron A 4000 D, Stuart. The values of CMC of surfactant solutions and equilibrium surface tension, σ_e at concentrations above CMC are given in Table 1.

The densities of studied solutions were measured by weighing 10 mL of solution dosed by Eppendorf pipette and were found to be similar to those of water for all surfactants solutions except C_{10}TAB at concentrations above CMC. However, the deviation of the density of C_{10}TAB at the maximum studied concentration 10 CMC from that of water was below 1% and therefore can be neglected. The viscosities of studied solutions were measured by a TA instruments Discovery-HR-2 rheometer in flow mode using cone and plate geometry with the angle 2^O 0′ 29″ and a truncation of 55 μm. Viscosities of solutions of C_{16}TAB were similar to that of water. Noticeable increase in viscosity was found only for solution C_{12}TAB, 10 CMC and C_{10}TAB 5 and 10 CMC (see Supplementary material, S1). The dynamic surface tension was measured using a maximum bubble pressure tensiometer BPA-1S (Sinterface, Germany).

The experiments were performed as follows: drops were formed continuously at the tip of stainless-steel capillary with outer radius R_{out} = 0.905 mm, inner radius R_{in} = 0.735 mm and length L_c = 43 mm at flow rates in the range from 0.1 mL/min to 40 mL/min using a syringe pump Al-4000, World Precision Instruments, UK. The syringe pump was equipped with 10 mL syringe (BD Plastipak^{TM}) for flow rates up to 10 mL/min and with 60 mL syringe for higher flow rates. The maximum Reynolds number in this study based on inner diameter of capillary, D_{in}, was $Re = \rho u D_{in}/\mu \sim 580$, i.e. flow conditions are well within the laminar flow regime. As the hydrodynamic entrance length $L_h = 0.05 Re D_{in}$ [21] ~ 42.5 mm for the maximum flow rate of 40 mL/min, fully developed flow is assumed at the capillary exit at all flow rates studied. Flow rate was changed always from lower to higher values and after any change in the flow rate, the system was left for 0.5–5 min for stabilisation depending on flow rate.

Table 1
Properties of surfactants used [17,20].

Surfactant	C_{10}TAB	C_{12}TAB	C_{16}TAB	C_{16}TAB + 10 mM NaBr
CMC, mM	60	15	0.9	0.1
σ_e, mN/m	39	39	37.5	37.2

Note, surface tension of PDMS is 17.2 mN/m, i.e. much lower than the minimum surface tension of all studied surfactant solutions.

Table 2
Characteristic numbers for the liquids under study.

Solution/ liquid	C_{10}TAB	C_{12}TAB	C_{16}TAB	C_{16}TAB + 10 mM NaBr	PDMS
Bo	0.11–0.21	0.11–0.21	0.11–0.22	0.11–0.22	0.38
Oh, 10^{-3}	3.9–9.4	3.9-7.8	3.9–5.4	3.9–5.5	7.3
We	10^{-5}–1.0	10^{-5}–1.0	10^{-5}–1.0	10^{-5}–2.5	$3{\cdot}10^{-5}$–1.1

The drop formation was followed using a Photron SA-5 high speed video-camera equipped with Navitar, 2X F-mount objective at 5000–42000 frames per second with a resolution of up to 4 μm/pixel.

Image processing was carried out using ImageJ and Matlab.

The characteristic numbers calculated for liquids under study are given in Table 2, where besides the aqueous surfactant solutions, PDMS is included in the last column. The range for surfactant solutions takes into account that the equilibrium surface tension changes from that of pure water to that given in Table 1 and viscosity changes according to S1. The calculation of the Weber numbers is based on equilibrium surface tension and takes into account that the flow rate increased until jetting regime was reached.

3. Results and discussion

3.1. Transition from dripping to jetting

For pure water transition from dripping to jetting was observed at flow rate 37 ± 1 mL/min which corresponds to a critical Weber number $We_J = 1.3$. This value is in line with scaling analysis performed in [5] showing that at $Oh << 1$, We_J should be $O(1)$. According to [4,5] We_J only weakly depends on Oh below $Oh < 0.02$ and at $Oh = 0.01$, $We_J \sim 0.8$ at $Bo = 0.5$ and $We_J \sim 1.2$ at $Bo = 0.3$. Considering that for water $Bo = 0.11$ and $Oh = 0.0039$, the obtained value of $We_J = 1.3$ is in good agreement with results of numerical simulations carried out in [4,5]. For PDMS our study gives $We_J \sim 1.1$. The small difference between We_J for water and PDMS is most probably due to difference in the values of Bond numbers, as it decreases with an increase of Bo. As all values of Bo and most values of Oh for studied surfactant solutions are in-between the values for water and PDMS, it is expected that for all surfactant solutions $We_J \sim$ 1.1-1.3.

Results on transition from dripping to jetting for surfactant solutions are presented in Fig. 1, where data for pure water and PDMS are also presented for comparison. Note, the values of the equilibrium surface tension for all considered solutions are close to each other at the same concentration normalised by CMC. For solutions of C_{10}TAB and C_{12}TAB the values of We_J based on equilibrium surface tension are in the expected range, but for solutions of C_{16}TAB at concentration 1 CMC and lower as well as for all solutions of C_{16}TAB + 10 mM NaBr, the transition takes place at considerably higher flow rates than expected from equilibrium surface tension. Therefore for these solutions dynamic surface tension should be taken into account [17]. The characteristic time scales for flow can be estimated as $t_f = R_{in}/u$ [5], being in the range of 20–30 ms for flow rates in the range of dripping to jetting transition, 20-35 mL/min. This estimation is in good agreement with values of time per drop (time span between the detachment of one main drop to that of the next main drop) just before the dripping to jetting transition found from the experiments (Fig. 2). Note, the experimental errors for data in Fig. 2 are rather large because drop formation before transition to jetting becomes less regular than in stationary dripping regime.

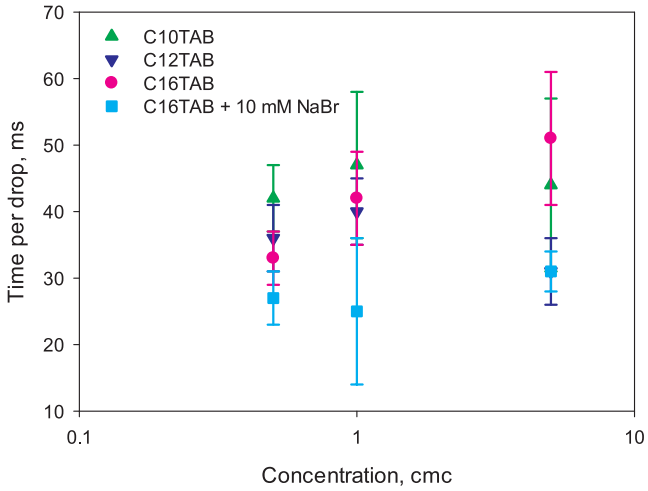

Fig. 2. Time per drop before transition from dripping to jetting.

Dynamic surface tension for solutions C_{12}TAB, C_{16}TAB and C_{16}TAB + 10 mM NaBr is presented in Figs. 3–5, respectively. According to Fig. 3, dynamic surface tension for the solution of C_{12}TAB on the timescale of flow at transition from dripping to jetting is very close to equilibrium surface tension. That is why transition is described quite well by critical Weber number based on equilibrium surface tension. The same is true for C_{10}TAB solutions. Solutions of C_{16}TAB at

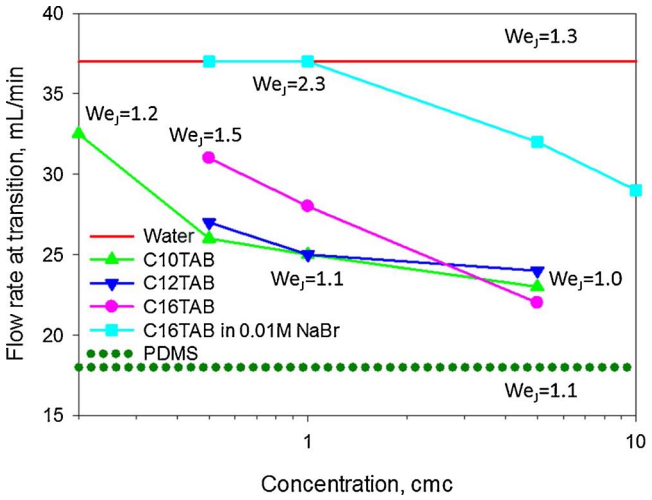

Fig. 1. Flow rates for transition from dripping to jetting for pure liquids and surfactant solutions. The values of Weber number at transition are based on equilibrium surface tension.

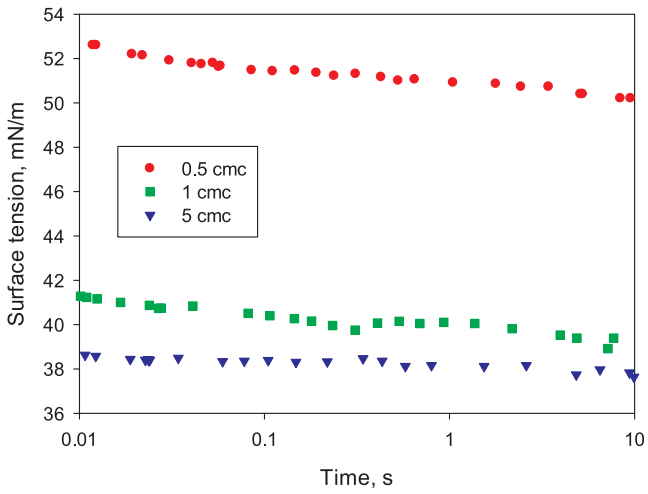

Fig. 3. Dynamic surface tension of solutions of C_{12}TAB at concentrations used in study of dripping to jetting transition. Equilibrium surface tension for concentration 0.5 cmc is ~49 mN/m.

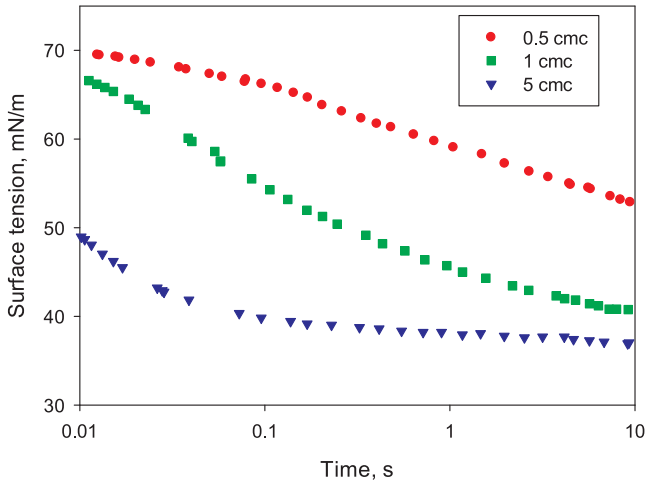

Fig. 4. Dynamic surface tension of solutions of C_{16}TAB at concentrations used in study of dripping to jetting transition.

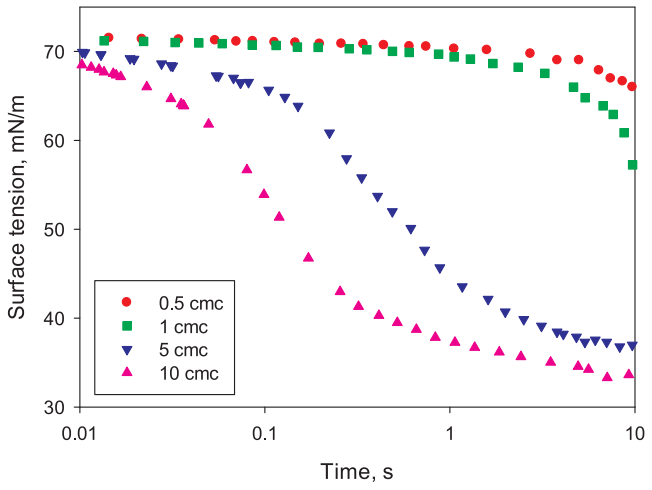

Fig. 5. Dynamic surface tension of solutions of C_{16}TAB + 10 mM NaBr at concentrations used in study of dripping to jetting transition.

concentrations c = 0.5 cmc and c = 1 cmc are rather far from equilibrium at the scale of t_f. Taking into account dynamic surface tension results in $We_J \sim 1.0$ for both c = 0.5 cmc and c = 1 cmc in good agreement with results for C_{10}TAB and C_{12}TAB. Surface tension of solutions C_{16}TAB + 10 mM NaBr at c = 0.5 cmc and c = 1 cmc are close to that of water, as is the transition flow rate. The dynamic surface tension still differs considerably from the equilibrium value at concentrations of 5 cmc and 10 cmc. Critical Weber numbers for these concentrations calculated by using dynamic surface tension are similar giving $We_J \sim 1.0$. Therefore it can be concluded that, under the conditions of this study, Weber number based on dynamic surface tension of surfactant solutions on the flow timescale describes reasonably well their transition from dripping to jetting.

3.2. Transition to regime without satellite droplets

3.2.1. Surfactant-free liquids

At small flow rates each main drop is accompanied by a satellite droplet. The latter forms because immediately before detachment of the main drop, the liquid filament connecting it with the liquid cone at the capillary has two necks, one near the main drop, and another near the capillary, called hereafter the top neck, (Fig. 6a, t = 0). After the primary pinch-off, when the main drop is released, the filament recoils whilst the secondary, top neck thins due to its larger capillary pressure when compared with the liquid cone and it eventually pinches off to form a satellite droplet (Fig. 6a, video S2 for PDMS).

With an increase in flow rate the liquid bridge between the capillary and the main drop becomes more elongated and the change in the radius between the filament and the cone becomes much less pronounced (sf. Fig. 6a–c at t = 0). Nevertheless even in the case presented in Fig. 6b (see S3 for the whole video) the difference in the capillary pressure between the filament and cone is high enough to produce a secondary pinch-off near the cone before the filament merges with the cone. However due to smaller difference in the capillary pressure and larger radius of the filament at transition to the cone, the time till secondary pinch-off increases from ~ 0.18 ms for water at a flow rate 0.1 mL/min (Fig. 6a) to ~ 0.45 ms at a flow rate 4.5 mL/min (Fig. 6b).

At higher flow rates the recoiling process happens faster than the thinning of the top neck near the liquid cone and the filament does not detach at this position. However, as is seen from Fig. 6, the recoiling produces a bulb and one more neck, called hereafter the bottom neck, at the bottom of the filament. At small flow rates, this bottom neck thins more slowly than the upper neck near the cone, but as the flow rate increases and the thinning of upper neck slows down, the secondary pinch-off moves from the top (Fig. 6b, S3) to the bottom neck (S4). For water, this transition occurs at Q = 5 mL/min (We = 0.025), whereas for PDMS it occurs at Q = 3 mL/min (We = 0.037). At flow rates close to the threshold for top to bottom pinch-off transition there is one more pinch-off producing a second satellite droplet (see S3 and S4). At higher flow rates the part of the filament left near the capillary merges with liquid cone and only one satellite is formed. This results in noticeable, 20–30 %, decrease of the size of satellite.

The kinetics of the bottom neck and the droplet connected to it (marked in Fig. 6) are a result of complex interplay between capillary pressure and inertia of the imposed liquid flow from the capillary. As is shown in Fig. 7, immediately after the primary pinch-off, the size of both neck and droplet increases due to recoiling. When the difference in size becomes large enough, the capillary pressure in the neck dominates and the neck diameter begins to decrease. The time interval between the primary pinch-off and beginning of the decrease of the diameter of the bottom neck increases with an increase of flow rate, i.e. with an increase of the flow rate a larger difference between the droplet and neck diameter is necessary for capillary pressure to overcome the liquid inertia. The rate of the neck thinning decreases with an increase of flow rate. At certain critical flow rate (7.9 mL/min in Fig. 7) inflow into neck exceeds the outflow due to capillary pressure and the neck begins to increase and the droplet eventually merges with the cone as shown in Fig. 6c (video S5 for PDMS).

For pure water, satellites disappear at flow rate $Q \sim 7.8 \pm 0.1$ mL/min (We_S = 0.06); for PDMS they disappear at $Q \sim 4.9$ mL/min (We_S = 0.10) as shown in Fig. 8. Calculations according to Eq. (4) give noticeably lower values of critical Weber number for transition to satellite free regime We_S = 0.03 for water and We_S = 0.018 for PDMS, giving lower value for PDMS than for water. This discrepancy could be due to the fact that our study was carried out for higher values of Ohnesorge number and lower values of Bond numbers than experimental study in [7]. The effect of Ohnesorge number was not considered in [7], whereas according to [6] critical Weber number depends considerably and non-linearly on the Ohnesorge number. In the present study, both Ohnesorge and Bond number change mainly due to change in the surface tension, therefore it is impossible to separate their contributions. Qualitatively it can be concluded that for the range of parameters of this study ($Bo < 0.4$, $Oh < 0.1$) a decrease in the surface tension results in an increase We_S for pure liquids. Since We_S for pure liquids depends on surface tension, we will consider this transition for surfactant solutions in terms of flow rate/surface tension, keeping in mind that for pure liquids the transitions flow rate Q_S decreases with a decrease of surface tension. The reference to Weber numbers will be given where appropriate.

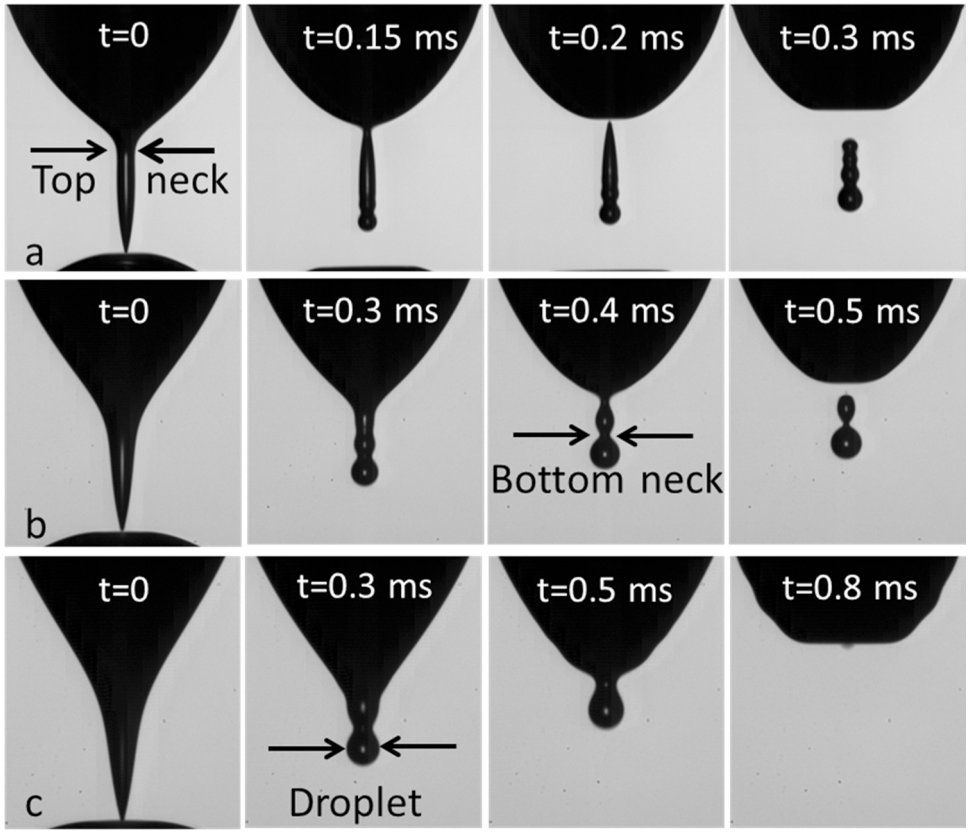

Fig. 6. Formation of satellite droplet by water dripping: a – Q = 0.1 mL/min, b – Q = 4.5 mL/min, c – Q = 7.9 mL/min; t = 0 corresponds to the primary pinch-off.

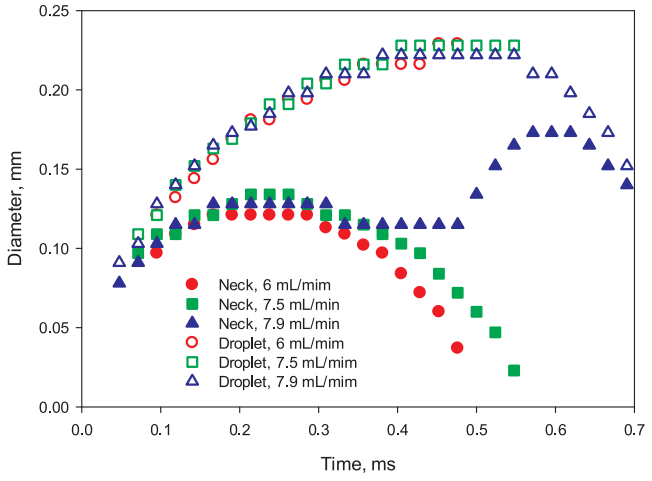

Fig. 7. Kinetics of droplets (empty symbols) and necks (filled symbols) formed at the bottom end of recoiling filament depending on flow rate; t = 0 corresponds to the primary pinch-off of the main drop.

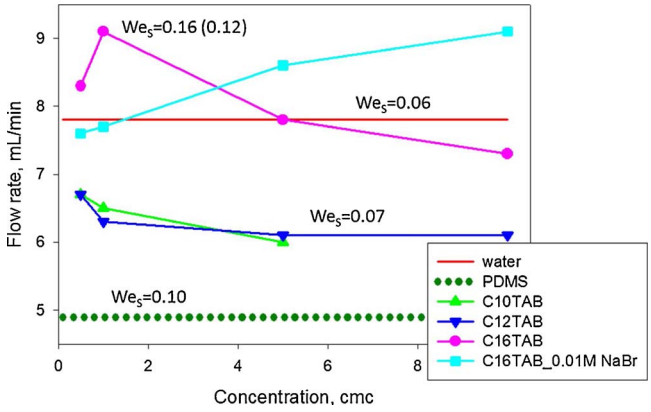

Fig. 8. Transition to regime without satellite droplets for pure liquids and surfactant solutions.

3.2.2. Surfactant solutions

It is seen from Fig. 8 that the data for solutions of C_{10}TAB and C_{12}TAB are in good agreement with the data for pure liquids. It was shown above that at transition from dripping to jetting these solutions behave similarly to pure liquids with surface tensions equal to the equilibrium values. Transition to the regime without satellite droplets occurs at considerably lower flow rates, i.e. at larger time scales. Fig. 9 presents the results for the timescale of drop formation for solutions of C_{12}TAB. According to Fig. 8 transition to the regime without satellite droplets for these solutions occurs between at 6 mL/min < Q < 7 mL/min. This gives timescale for formation of the main drop ~ 0.17 s. Dynamic surface tension at this timescale (Fig. 3) is equal to the equilibrium value for micellar solutions and close to equilibrium for c = 0.5 cmc. That is why solutions of C_{10}TAB and C_{12}TAB behave like pure liquids (without any dynamic effects related to surfactant redistribution) also in transition to regime without satellite droplets.

The situation changes for solutions with slower equilibration rate, C_{16}TAB and C_{16}TAB + 10 mM NaBr (Figs. 4 and 5). Transition occurs at even higher flow rates than those for pure water for C_{16}TAB at c < 5 CMC and C_{16}TAB + 10 mM NaBr at c > 2 CMC. We_S for these solutions based on dynamic surface tension at the corresponding time scale is considerably higher than that for C_{10}TAB and C_{12}TAB. For 1 CMC solution of C_{16}TAB and 10 CMC solution of C_{16}TAB + 10 mM NaBr dynamic surface tension on the time scale of drop formation at transition (0.17–0.21 s) is ~44–50 mN/m, giving We_S = 0.12-0.13, even higher than We_S for PDMS. Moving of the secondary pinch-off from the top (near the capillary) to the bottom (at the bottom of filament) position

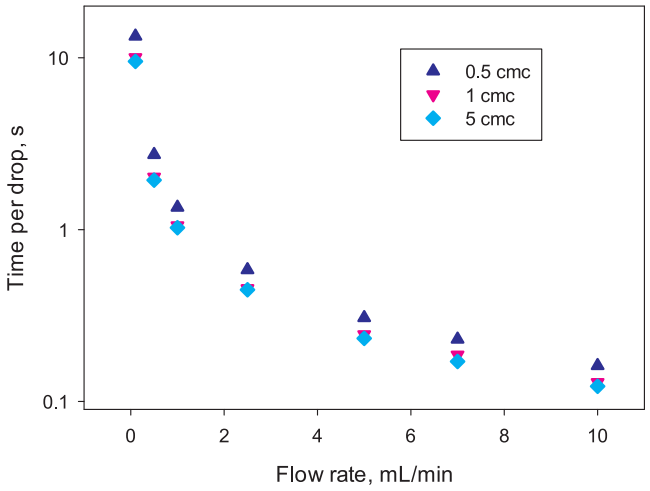

Fig. 9. Time per drop for solutions of C_{12}TAB depending on flow rate. In the studied range of flow rates the drop size only slowly increases with flow rate and time per drop $t \sim Q^{-0.94 \pm 0.01}$.

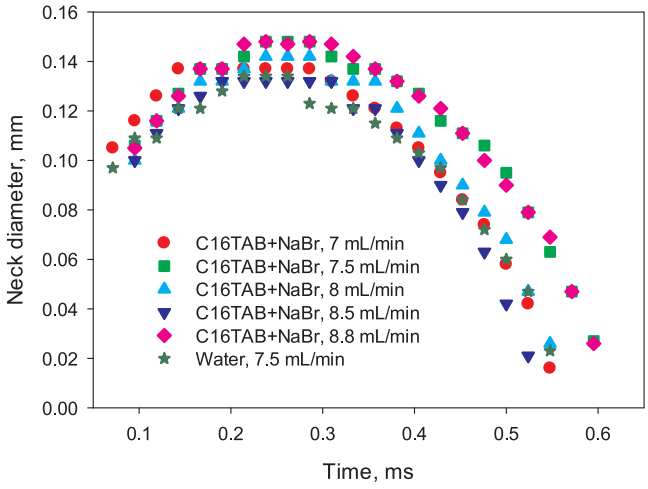

Fig. 11. Time dependence of the diameter of the secondary neck before secondary pinch-off for water and 10 CMC solution of C_{16}TAB + 10 mM NaBr at various flow rates.

for these solutions also occurs at higher flow rate than for pure water. For example, for solution of 5 CMC of C_{16}TAB + 10 mM NaBr, this transition was observed at Q = 6.5 mL/min.

Comparison of recoiling rate of surfactant solutions and pure water (as found from the slope of linear fitting of curves in Fig. 10) shows that at the same flow rate, Q = 6 mL/min, the recoiling rate for solution of C_{12}TAB is slower than that of water with recoiling rate ratio being ~ 1.4. At the same time the thinning of the secondary neck also slows down due to smaller capillary pressure in the surfactant solution. The time between the primary and secondary pinch-off increases from 0.5 ms for water to 1 ms for solution of 10 CMC of C_{12}TAB, i.e. neck thinning slows more than recoiling. As a result, transition to the regime without satellite drops moves to a lower flow rate.

For solution of C_{16}TAB + 10 mM NaBr, 10 CMC the dynamic surface tension in the range of flow rates 7–10 mL/min (based on time per drop 0.17–0.21 s) is 44–50 mN/m (Fig. 5). However the recoiling rate is similar to that of water (Fig. 10) indicating the depletion of surfactant from the pinch-off region during the bridge thinning [16,17,22,23], resulting in a surfactant concentration at the neck at the moment of pinch-off close to zero. At the same time the surface tension in the parts of the filament away from the neck should be lower, because the surfactant is transferred there from the pinch-off region. Indeed, it is seen from Fig. 11 that the neck thinning at the same flow rate, 7.5 mL/min, takes longer and the maximum neck diameter is larger for 10 CMC solution of C_{16}TAB + 10 mM NaBr than for water, indicating that lower surface tension is acting at the secondary neck for surfactant solutions.

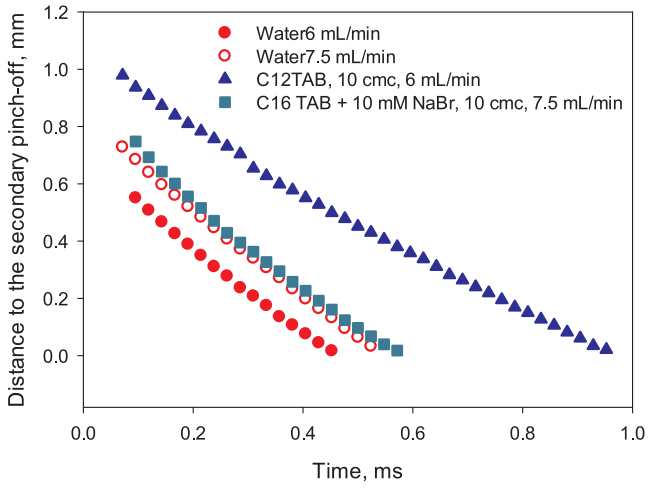

Fig. 10. Recoiling of pure water and surfactant solutions after primary pinch-off.

For pure water the bottom neck thinning slows down with an increase of flow rate (Fig. 7), as does the neck thinning for 10 CMC solution of C_{16}TAB + 10 mM NaBr at flow rates up to 7.5 mL/min. However, the thinning kinetics accelerates when the flow rate increases above 7.5 mL/min. The maximum rate of thinning was observed at Q = 8.5 mL/min. Afterwards it begins to slow down with the increase of flow rate with kinetics at Q = 8.8 mL/min being the same as at Q = 7.5 mL/min. This anomaly in dependence of thinning kinetics on flow rate is the reason for the higher flow rates needed for transition to the regime without satellites. The anomaly in turn is the result of further surfactant redistribution inside the filament. The accelerated thinning kinetics indicates surfactant depletion from the secondary neck at higher flow rates. However, this acceleration stops when the surface tension at the neck becomes equal to that of pure water (at Q = 8.5 mL/min). After that deceleration takes place as was observed earlier for pure liquids.

The difference in the behaviour of surfactant solutions with high and low CMC values is related to the difference in equilibration rates as shown in Figs. 3–5. Surfactant with larger CMC equilibrates faster at the same concentration normalised by CMC (i.e. at the similar equilibrium surface tension) because of larger dimensional concentration and therefore larger concentration gradients for the same change in the surface tension. Another (less important) reason can be larger diffusion coefficients of monomers and micelles for surfactants with shorter chain length. For example the diffusion coefficient for monomers of C_{10}TAB estimated according to the Wilke-Chang correlation [24] is $4.5 \cdot 10^{-10}$ m^2/s, whereas that for C_{16}TAB is $3.7 \cdot 10^{-10}$ m^2/s. Therefore the dynamic effects are less important for surfactants with high CMC values. According to this study the dynamic effects can be neglected at CMC > 10 mM, but they should be always taken into account at CMC < 1 mM. C_{16}TAB equilibrates faster than C_{16}TAB + 10 mM NaBr at the same normalised concentration. That is why the maximum flow rate at transition to regime without satellite droplets is observed for C_{16}TAB at concentration 1 CMC, whereas for C_{16}TAB + 10 mM NaBr only at concentration ≥ 10 CMC.

4. Conclusions

Transition from dripping to jetting, formation of satellite droplets in dripping regime and transition to regime without satellites was studied for water, low viscosity poly(dimethylsiloxane) and aqueous solutions of alkyltrimethylammonium bromides with chain length C10-C16 in concentration range 0.2–10 CMC.

Transition from dripping to jetting in surfactant solutions under condition Oh $<<$ 1 and low viscosity of ambient fluid is governed by Weber number calculated using dynamic surface tension on the flow timescale. The critical Weber number for this transition is $We_J = 1.2 \pm 0.1$. Effect of gravitational Bond number is rather weak in the range of $0.1 < Bo < 0.4$.

At small flow rates, dripping from a capillary is accompanied by formation of satellite droplets. An increase in the flow rate results in the change of position of the secondary pinch-off from the top of the liquid filament to its bottom and finally in transition to the regime without satellite droplets. The Weber number of this transition depends on surface tension and therefore is not used for transition characterisation. The flow rate for the transition to the regime without satellite droplets decreases with a decrease of surface tension for pure liquids. The solutions of surfactants with high values of CMC $>$ 10 mM behave similarly to pure liquids with surface tension equal to the equilibrium surface tension.

For solutions of surfactants with CMC $<$ 1 mM the flow rate at transition to the regime without satellites can be either larger or smaller than that of pure solvent depending on concentration. The range of concentrations at which transition to the regime without satellite droplets occur at higher flow rates than for the solvent increases with a decrease of CMC value. Those anomalously high transition flow rates are related to surfactant redistribution during the time between the primary and secondary pinch-off.

Acknowledgements

This work is funded by the EPSRC Programme Grant “MEMPHIS – Multiscale Examination of Multiphase Physics in Flows” (EP/K003976/1).

Appendix A. Supplementary data

Supplementary material related to this article can be found, in the online version, at doi:https://doi.org/10.1016/j.colsurfa.2018.02.041.

References

[1] J. Eggers, E. Villermaux, Physics of liquid jets, Rep. Prog. Phys. 71 (3) (2008).
[2] C. Clanet, J.C. Lasheras, Transition from dripping to jetting, J. Fluid Mech. 383 (1999) 307–323.
[3] J. Eggers, Nonlinear dynamics and breakup of free-surface flows, Rev. Mod. Phys. 69 (3) (1997) 865–929.
[4] H.J. Subramani, et al., Simplicity and complexity in a dripping faucet, Phys. Fluids 18 (3) (2006) 032106.
[5] B. Ambravaneswaran, et al., Dripping-jetting transitions in a dripping faucet, Phys. Rev. Lett. 93 (3) (2004) 034501.
[6] B. Ambravaneswaran, E.D. Wilkes, O.A. Basaran, Drop formation from a capillary tube: comparison of one-dimensional and two-dimensional analyses and occurrence of satellite drops, Phys. Fluids 14 (8) (2002) 2606–2621.
[7] X. Zhang, Dynamics of growth and breakup of viscous pendant drops into air, J. Colloid Interface Sci. 212 (1999) 107–122.
[8] S.D. Hoath, et al., How PEDOT:PSS solutions produce satellite-free inkjets, Org. Electron. 13 (12) (2012) 3259–3262.
[9] W.D. Wu, et al., Monodisperse droplet Generators as potential atomizers for spray drying technology, Drying Technol. 25 (12) (2007) 1907–1916.
[10] N. Bremond, et al., Formation of liquid-core capsules having a thin hydrogel membrane: liquid pearls, Soft Matter 6 (11) (2010) 2484–2488.
[11] H. Domejean, et al., Controlled production of sub-millimeter liquid core hydrogel capsules for parallelized 3D cell culture, Lab Chip 17 (2017) 110–119.
[12] X. Zhang, O.A. Basaran, An experimental study of dynamics of drop formation, Phys. Fluids 7 (6) (1995) 1184–1203.
[13] P.K. Notz, A.U. Chen, O.A. Basaran, Satellite drops: unexpected dynamics and change of scaling during pinch-off, Phys. Fluids 13 (3) (2001) 549–552.
[14] B. Ambravaneswaran, O.A. Basaran, Effects of insoluble surfactants on the nonlinear deformation and breakup of stretching liquid bridges, Phys. Fluids 11 (5) (1999) 997–1015.
[15] R.V. Craster, O.K. Matar, D.T. Papageorgiou, Pinchoff and satellite formation in surfactant covered viscous threads, Phys. Fluids 14 (4) (2002) 1364–1376.
[16] R.V. Craster, O.K. Matar, D.T. Papageorgiou, Breakup of surfactant-laden jets above the critical micelle concentration, J. Fluid Mech. 629 (2009).
[17] N.M. Kovalchuk, E. Nowak, M.J. Simmons, Effect of soluble surfactants on the kinetics of thinning of liquid bridges during drops formation and on size of satellite droplets, Langmuir 32 (20) (2016) 5069–5077.
[18] N.M. Kovalchuk, E. Nowak, M.J.H. Simmons, Kinetics of liquid bridges and formation of satellite droplets: difference between micellar and bi-layer forming solutions, Colloids Surf. A: Physicochem. Eng. Asp. 521 (2017) 193–203.
[19] F. Jin, N.R. Gupta, K.J. Stebe, The detachment of a viscous drop in a viscous solution in the presence of a soluble surfactant, Phys. Fluids 18 (2) (2006).
[20] V. Bergeron, Disjoining pressures and film stability of alkyltrimethylammonium bromide foam films, Langmuir 13 (1997) 3474–3482.
[21] F.P. Incropera, et al., Fundamentals of Heat and Mass Transfer, 6th ed., John Wiley & Sons, 2007, p. 997.
[22] M. Roche, et al., Effect of surface tension variations on the pinch-off behavior of small fluid drops in the presence of surfactants, Phys. Rev. Lett. 103 (26) (2009) 264501.
[23] M.R. de Saint Vincent, et al., Dynamic interfacial tension effects in the rupture of liquid necks, J. Fluid Mech. 692 (2012) 499–510.
[24] B.E. Poling, J.M. Prausnitz, J.P. O’connel, The Properties of Gases and Liquids, McGraw-Hill, 2001.